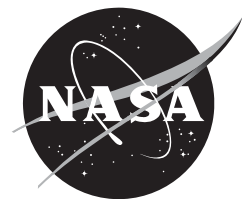


NASA/TM—2014—218366



Conceptual Launch Vehicle and Spacecraft Design for Risk Assessment

Samira A. Motiwala
Stanford University, Stanford, CA, 94305

Donovan L. Mathias
NASA Ames Research Center, Moffett Field, CA 94035

Christopher J. Mattenberger
Science and Technology Corporation, Moffett Field, CA 94035

June 2014

NASA STI Program ... in Profile

Since its founding, NASA has been dedicated to the advancement of aeronautics and space science. The NASA scientific and technical information (STI) program plays a key part in helping NASA maintain this important role.

The NASA STI program operates under the auspices of the Agency Chief Information Officer. It collects, organizes, provides for archiving, and disseminates NASA's STI. The NASA STI program provides access to the NTRS Registered and its public interface, the NASA Technical Reports Server, thus providing one of the largest collections of aeronautical and space science STI in the world. Results are published in both non-NASA channels and by NASA in the NASA STI Report Series, which includes the following report types:

- **TECHNICAL PUBLICATION.** Reports of completed research or a major significant phase of research that present the results of NASA Programs and include extensive data or theoretical analysis. Includes compilations of significant scientific and technical data and information deemed to be of continuing reference value. NASA counterpart of peer-reviewed formal professional papers but has less stringent limitations on manuscript length and extent of graphic presentations.
- **TECHNICAL MEMORANDUM.** Scientific and technical findings that are preliminary or of specialized interest, e.g., quick release reports, working papers, and bibliographies that contain minimal annotation. Does not contain extensive analysis.
- **CONTRACTOR REPORT.** Scientific and technical findings by NASA-sponsored contractors and grantees.

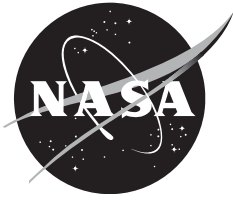
- **CONFERENCE PUBLICATION.** Collected papers from scientific and technical conferences, symposia, seminars, or other meetings sponsored or co-sponsored by NASA.
- **SPECIAL PUBLICATION.** Scientific, technical, or historical information from NASA programs, projects, and missions, often concerned with subjects having substantial public interest.
- **TECHNICAL TRANSLATION.** English-language translations of foreign scientific and technical material pertinent to NASA's mission.

Specialized services also include organizing and publishing research results, distributing specialized research announcements and feeds, providing information desk and personal search support, and enabling data exchange services.

For more information about the NASA STI program, see the following:

- Access the NASA STI program home page at <http://www.sti.nasa.gov>
- E-mail your question to help@sti.nasa.gov
- Phone the NASA STI Information Desk at 757-864-9658
- Write to:
NASA STI Information Desk
Mail Stop 148
NASA Langley Research Center
Hampton, VA 23681-2199

NASA/TM—2014—218366



Conceptual Launch Vehicle and Spacecraft Design for Risk Assessment

Samira A. Motiwala
Stanford University, Stanford, CA, 94305

Donovan L. Mathias
NASA Ames Research Center, Moffett Field, CA

Christopher J. Mattenberger
Science and Technology Corporation, Moffett Field, CA 94035

June 2014

Acknowledgments

The student author would like to thank her mentors, Donovan Mathias and Chris Mattenberger, as well as Ken Gee, Lorien Wheeler, and Susie Go for their extensive help and patience. The student author would also like to acknowledge the California Space Grant Consortium and the NASA Education Associates Program (EAP) for their financial support.

Available from:

NASA Center for AeroSpace Information
7115 Standard Drive
Hanover, MD 21076-1320
443-757-5802

This report is also available in electronic form at
<http://www.ntrs.nasa.gov>

Table of Contents

Nomenclature.....	6
1. Introduction	6
2. Preliminary Spacecraft Sizing	6
2.1. Mass and Power Estimation	7
2.2. Geometry.....	9
3. Launch Vehicle Sizing and Trajectory Analysis	10
3.1. Design Assumptions.....	10
3.2. Optimal Staging.....	11
3.3. Inboard Sizing.....	11
3.4. Initial Two-Stage-to-Orbit Trajectory Analysis	12
3.5. Optimal Trajectory Analysis.....	14
3.6. Final Launch Vehicle Design.....	16
4. Concept of Operations	17
5. Spacecraft Subsystems Layout.....	17
5.1. Structures and Mechanisms	18
5.2. Thermal Control System.....	20
5.3. Environmental Control and Life Support System (ECLSS).....	22
5.4. Power.....	24
5.5. Avionics	26
5.6. Propulsion.....	28
5.7. Crew Accommodations	30
5.8. Entry, Descent, and Landing (EDL)	30
5.9. Spacecraft Subsystem Summary	31
6. Safety Design and Risk Analysis	31
6.1. Spacecraft Reliability	32
6.2. Launch Vehicle Reliability	34
7. Summary.....	35
References	35

Nomenclature

γ = flight path angle, correlation factor γ_e = flight path angle at entry interface Δv = velocity increment ε = structural fraction coefficient λ = failure rate μ = standard gravitational parameter ν = true anomaly π = payload fraction ω = argument of perigee Ω = right ascension of ascending node a = acceleration, semi-major axis A_e = exit area A_t = throat area c = effective velocity cm = center of mass cp = center of pressure d = diameter D = drag, mission duration e = eccentricity E = modulus of elasticity f_{cu} = ultimate compressive stress F_{cr} = elastic buckling stress F_{tu} = ultimate tensile stress F_{ty} = yield tensile stress g = gravitational acceleration g_0 = gravitational acceleration at sea level h = altitude/height h_e = altitude at entry interface h_{fg} = latent heat of vaporization h_i = altitude of initial circular orbit or parking orbit I = moment of inertia I_{sp} = specific impulse J = cost function	LH_2 = liquid hydrogen LOX/LO_2 = liquid oxygen m = mass m_0 = total mass m_{bo} = burnout mass m_{GLOM} = gross lift-off mass m_{inert} = inert mass m_{prop} = propellant mass m_{stage} = stage mass M_e = expendable mass M_{max} = peak bending moment n = load factor p_u = ultimate internal pressure p_y = yield internal pressure P_{avg} = average power P_c = chamber pressure, compressive axial force P_{peak} = peak power q = dynamic pressure Q = heat rejection rate r = radius r_{eq}, R_E = Earth equatorial radius R = reliability $RP-1$ = Rocket Propellant-1 (kerosene) t = time t_1, t_2, t_3 = thickness T = thrust T/W = thrust-to-weight ratio u = thrust directional control v = velocity V_{ce} = local circular velocity at entry interface x = downrange distance
---	--

1. Introduction

One of the most challenging aspects of developing human space launch and exploration systems is minimizing and mitigating the many potential risk factors to ensure the safest possible design while also meeting the required cost, weight, and performance criteria. In order to accomplish this, effective risk analyses and trade studies are needed to identify key risk drivers, dependencies, and sensitivities as the design evolves. The Engineering Risk Assessment (ERA) team at NASA Ames Research Center (ARC) develops advanced risk analysis approaches, models, and tools to provide such meaningful risk and reliability data throughout vehicle development. The goal of the project presented in this memorandum is to design a generic launch

vehicle and spacecraft architecture that can be used to develop and demonstrate these new risk analysis techniques without relying on other proprietary or sensitive vehicle designs.

To accomplish this, initial spacecraft and launch vehicle (LV) designs were established using historical sizing relationships for a mission delivering four crewmembers and equipment to the International Space Station (ISS). Mass-estimating relationships (MERS) were used to size the crew capsule and launch vehicle, and a combination of optimization techniques and iterative design processes were employed to determine a possible two-stage-to-orbit (TSTO) launch trajectory into a 350-kilometer orbit. Primary subsystems were also designed for the crewed capsule architecture, based on a 24-hour on-orbit mission with a 7-day contingency. Safety analysis was also performed to identify major risks to crew survivability and assess the system's overall reliability. These procedures and analyses validate that the architecture's basic design and performance are reasonable to be used for risk trade studies. While the vehicle designs presented are not intended to represent a viable architecture, they will provide a valuable initial platform for developing and demonstrating innovative risk assessment capabilities.

2. Preliminary Spacecraft Sizing

An initial spacecraft design begins with a rough assessment of the requirements and scope of its intended mission. NASA is currently administering its Commercial Crew Program (CCP), a multiphase program intended to help the US industry develop space transportation systems to safely launch astronauts and cargo to the ISS and other low-Earth orbit destinations¹. The generic space vehicle system designed here will apply the same requirements defined for the CCP, which include delivering four crew members and their equipment to the ISS while ensuring safety in the event of an emergency on the pad or during launch and ascent. In addition, the spacecraft is expected to demonstrate its ability to serve as a 24-hour safe haven during an on-orbit emergency¹, but the design presented here will include a 7-day contingency as well.

2.1. Mass and Power Estimation

Conceptual design of this spacecraft begins with estimating the pressurized volume required by the crew, which can be determined from historical guidelines based on mission duration, as shown in Figure 1.

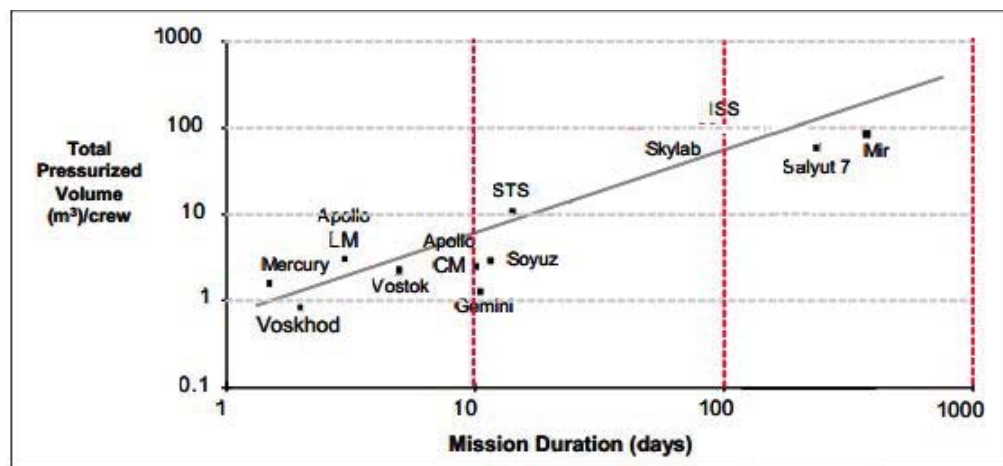


Figure 1. Pressurized volume as a function of mission duration with historical reference cases².

Applying this guideline to a 7-day mission yields roughly 4 m³ of pressurized volume per person, or 16 m³ of total pressurized volume. After the crew compartment volume is determined, a first estimate of the vehicle's burnout mass (m_{bo}) can be calculated based on historical data for human spacecraft using the following equation³:

$$m_{bo}[kg] = 592 \times (\#crew \times mission\ duration [d] \times pressurized\ volume [m^3])^{0.346} \quad (1)$$

The total dry mass of the spacecraft module consists of the burnout mass and the entry, descent, and landing (EDL) mass, which can be estimated as 15-18% of the burnout mass⁴. Propellant mass (m_{prop}) may be determined from the ideal rocket equation:

$$m_{prop} = m_{bo} \left(e^{\left(\frac{\Delta v}{I_{sp} g} \right)} - 1 \right) \quad (2)$$

The velocity increment, Δv , required for this mission consists of the velocity increment needed to deorbit as well as a 50% margin for emergency maneuvers, orbital corrections, and orbital decay. A standard storable liquid propulsion system using monomethylhydrazine and nitrogen tetroxide (MMH/NTO) is assumed, with a specific impulse of 310 seconds. As a general guideline, the mass of the propulsion system without the propellant (tanks, lines, engines, etc.) can be estimated as 15% of the propellant mass⁴ and is included back in the original burnout mass. This process repeats for a few iterations until a near convergent solution is reached.

Deorbit Δv can be determined from the following equation⁵:

$$\Delta v_{deorbit} = V_{ce} \sqrt{\frac{1}{r}} \left\{ 1 - \sqrt{\frac{2(r-1)}{\left(\frac{r}{\cos \gamma_e} \right)^2 - 1}} \right\} \quad (3)$$

where

$$r = \text{radius ratio} = \frac{h_i + r_{eq}}{h_e + r_{eq}} \quad (4)$$

Parameters required to estimate deorbit Δv (flight path angle and altitudes) were taken from Space Shuttle values⁵ as a best estimate, and the total Δv required (with a 50% margin) was estimated to be about 197.5 m/s.

After estimating the spacecraft's total dry mass, each of its subsystems need to be defined and allocated a percentage of the dry mass (using MERs) to obtain a first-order mass estimate. These subsystems include: structure and mechanisms, thermal control, environmental control and life support system (ECLSS), power, avionics/communications, attitude determination and control, crew accommodations, propulsion, EDL, and the payload (astronaut crew and suits). Payload is assumed to be 90 kg (~200 lb) for each person and 50 kg (~110 lb) for each suit system⁶.

After the inert mass has been determined, a design margin of 25% is added to all subsystems to enable room for mass growth, and wet mass (propellant and other consumables) is added to the mass budget. Finally, the LAS mass is included, and is estimated to be roughly 70% of the

inert mass* (with margin). The total mass of the spacecraft with LAS was determined to be about 13,800 kg. Table 1 provides a mass breakdown of the spacecraft’s main subsystems and other components.

Table 1. Preliminary mass budget for spacecraft design.

Subsystem	% Dry Mass	Mass (kg)	With 25% Margins (kg)
Structure	22	1,251	1,564
Mechanisms	8	455	569
Thermal Control	9	512	640
ECLSS	8	455	569
Power	15	853	1,066
Avionics	10	569	711
ADCS/GNC	2	114	142
Crew Accommodations	8	455	569
EDL	18	1,023	1,279
TOTAL DRY (W/O PROPULSION)	100	5,686	7,107
Propulsion	-	50	-
Payload (Crew with Suits)	-	560	-
TOTAL DRY (INERT)	-	7,667	
Main Propellant	-	332	-
Propellant for ADCS	-	213	
Consumables	-	224	-
TOTAL SPACECRAFT	-	8,436	
Launch Abort System	-	5,367	-
GROSS MASS		13,803	

Power budgets for space vehicles vary depending on mission requirements, but general guidelines⁴ for estimating the average and peak power required are:

$$P_{avg} = 1000 \text{ W} + 500 \text{ W} \times \text{number of crew} \quad (5)$$

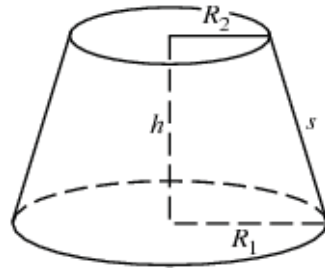
$$P_{peak} = P_{avg} \times 1.75 \quad (6)$$

These estimates yield average and peak power requirements of 3 kW and 5.25 kW, respectively.

2.2. Geometry

The spacecraft command module (CM) is assumed to be a conical frustum with the corresponding parameters shown in Figure 2. The service module (SM) is estimated as a cylindrical shell with the same large diameter and a height of 3 meters. Inertia properties can be found in Table 11(a) in section 5.5.

* Based on 2 previous existing abort systems and guideline provided by INTROS⁷



Parameter	Value	Units
Radius R_1	2.5	m
Radius R_2	0.1	m
Height h	3.5	m
Slant Height s	4.24	m
Surface Area	54.3	m ²
Volume	23.9	m ³

Figure 2. Command module geometry.

3. Launch Vehicle Sizing and Trajectory Analysis

Sizing a launch vehicle can involve many different approaches and employ a variety of mass-estimating techniques. The architecture developed here uses a top-down approach involving optimal staging to size the inert and propellant stage masses (based on assumptions), designing the inert stage components (tanks, engines, etc.), and then comparing their masses to estimated ones, analyzing a rough trajectory performance to determine feasibility, and iterating multiple times until a closed, satisfactory solution is reached.

3.1. Design Assumptions

A TSTO launch vehicle is assumed since it is the most common and practical design. A single-stage vehicle is not practical for achieving higher burnout velocities, and three (or more) stages provide unnecessary extra performance for added weight⁸ and risk penalties from increased complexity. The launch vehicle must generate enough Δv to meet mission requirements and place the spacecraft into orbit while accounting for gravity and drag losses and possible launch site gains. The spacecraft's speed at orbital insertion must match the speed required to maintain the selected orbit. It is assumed that the vehicle will launch from Cape Canaveral (28.5° latitude) into a 350-km circular orbit at an inclination of 51.6 degrees to dock with the ISS, and will therefore require a total design Δv of about 9.5 km/s⁸.

Other assumptions include propellant types (fuels and oxidizers), specific impulses, structural mass fractions, thrust-to-weight ratios, and number of engines for each stage. Table 2 summarizes the launch vehicle assumption parameters.

Table 2. TSTO launch vehicle assumptions.

Stage	Propellant	Specific Impulse (s)	Structural Mass Fraction*	T/W*	# Engines
1	Lox/RP-1	350	0.06	1.3	4
2	Lox/LH ₂	450	0.1	0.75	2

*Initial assumption (changes with iterations)

3.2. Optimal Staging

Sizing each stage while minimizing the total LV mass requires an optimal staging technique that utilizes the Lagrange multiplier method, a mathematical optimization strategy for solving the local maxima and minima of a given bivariate function subject to certain constraints[†]. This technique involves defining the specific impulse and structural mass fraction of each stage, payload mass, and design Δv to yield the minimum-mass N -stage vehicle to carry that payload into orbit. This method is in contrast to the restricted staging assumption that all stages of a tandem-stacked vehicle are similar and should be designed with the same specific impulse, payload ratio, structural mass fraction, and consequently, mass ratio⁹.

3.3. Inboard Sizing

After an initial sizing of all stages is complete, the LV inboard profile is considered. This includes deciding how all LV components (engines, tanks, attachments, etc.) will fit into a given envelope. Sizing procedures involve choosing the LV geometry, dimensionalizing the components, and using MERs for all components to determine the vehicle's total expected inert mass⁸.

Three iterations were initially carried out to achieve a positive design margin between expected stage inert masses (from optimal staging) and calculated stage inert masses (from inboard sizing). The first iteration assumed spherical tanks (which require a large diameter) and yielded a large negative design margin. The second iteration scaled the LV diameter down to 4 m while resizing the propellant tanks (to cylindrical shells with spherical domes) to fit. This improved the margin significantly because it reduced the required fairing surface area, thus reducing mass. However, the margin was still negative, and the diameter can only be decreased so much before the LV is considered infeasible due to structural complications. The third iteration experimented with different structural mass fractions[‡] for each stage until a positive design margin was achieved. Generally, higher structural mass fractions yield heavier vehicles, so these fractions were chosen to be as low as possible while still yielding a design margin of about 10%.

Engines were sized by assuming a telescopic, crank-down nozzle for each engine, with an 80% nozzle length and 15° cone divergent, 30° convergent half-angles. Guidelines exist⁸ for estimating the characteristic chamber length (0.75 m) and the ratio of the chamber length to diameter (typically 0.9 m). In addition, typical parameters associated with different fuel and oxidizer combinations can be found in Table 3⁸.

Table 3. Typical engine parameters.

Parameter	Stage 1 LOX/RP-1	Stage 2 LOX/LH ₂
Chamber Pressure, P_c (psi)	3,000	2,500
Expansion Ratio (A_e/A_t)	30	150
Theoretical c (m/s)	1,825	2,325
Delivered c (m/s)	1,789	2,279

[†] See Curtis⁹ section 11.6.1 (“Lagrange Multiplier”) for more information

[‡] Typical structural mass fractions range from 0.038 to 0.45, based on historical data¹⁰

3.4. Initial Two-Stage-to-Orbit Trajectory Analysis

The LV trajectory analysis was initially conducted with a simple gravity turn trajectory, where the launch vehicle takes off vertically and gradually transitions into horizontal flight at orbital insertion⁸⁻⁹. The ascent was separated into three phases: first stage propellant burn and separation, second stage ignition and LAS ejection 30 seconds later, and second stage propellant burn and separation prior to orbital insertion. Performance assumptions include constant thrust during burn with no steering losses. A five-second coast period was also assumed between propellant burnout and stage separation (for both stages), with no thrust during the coast. Aerodynamic assumptions included a drag coefficient of 0.2 and a reference area calculated from the 4-m diameter cross-section.

Figure 3 illustrates a simplified free-body diagram of the launch vehicle in flight. A vertical liftoff is followed by a small “kick” in the flight path angle after the launch vehicle clears the tower, which is usually around 100–150 m⁹.

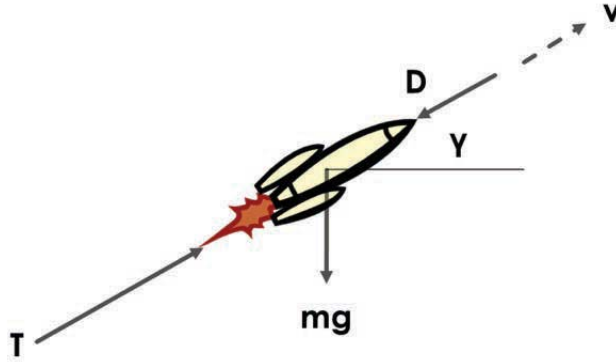


Figure 3. Simplified launch vehicle free-body diagram for gravity-turn trajectory.

Equations (7) to (10) are the primary coupled equations of motion⁸⁻⁹ to propagate and iterate until a satisfactory convergent solution is reached. These equations account for the aforementioned losses and Δv boost obtained from launching due east in order to achieve the 7.7 km/s circular orbit velocity at insertion.

$$\frac{dv}{dt} = \frac{T}{m} - \frac{D}{m} - g \sin \gamma \quad (7)$$

$$v \frac{d\gamma}{dt} = - \left(g - \frac{v^2}{R_E + h} \right) \cos \gamma \quad (8)$$

$$\frac{dx}{dt} = \frac{R_E}{R_E + h} v \cos \gamma \quad (9)$$

$$\frac{dh}{dt} = v \sin \gamma \quad (10)$$

Figure 4 and Figure 5 display the primary results obtained from this basic trajectory analysis. The performance parameters presented include the flight path angle (degrees), acceleration (m/s^2), velocity ($\times 10 \text{ km/s}$), altitude (km), and dynamic pressure ($\times 0.01 \text{ Pa}$). The 2D spatial trajectory of altitude vs. downrange distance is also presented. The initial kick from the flight path angle was determined to be 0.3 degrees ($\gamma_i \approx 89.7 \text{ degrees}$) and the total time of flight was estimated to be about 550 seconds. The gravity-turn trajectory served as a precursor to optimal trajectory analysis, where a good first guess is required to achieve a desired solution.

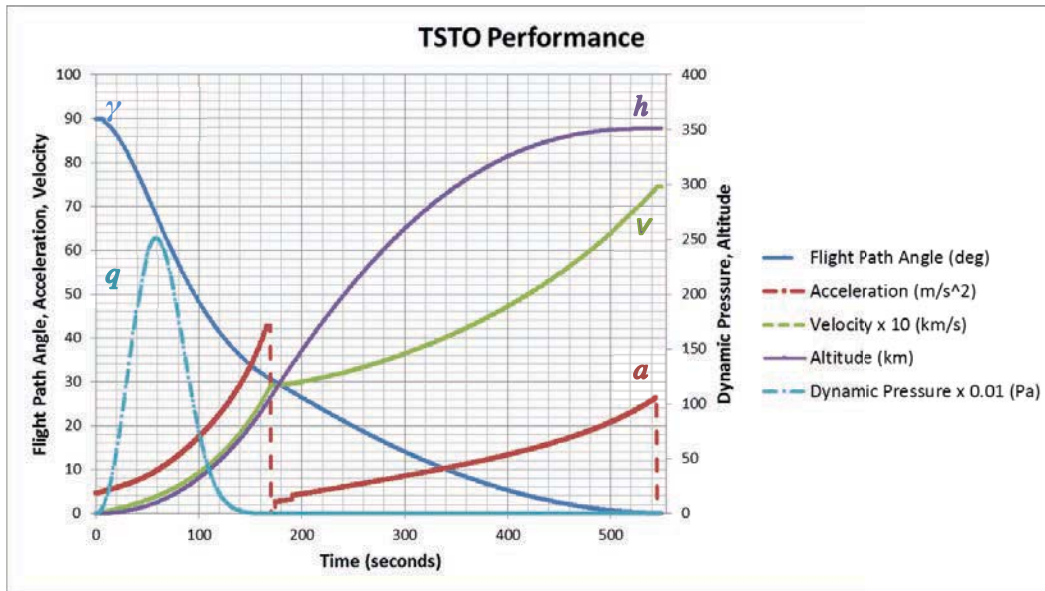


Figure 4. Two-stage-to-orbit performance results.

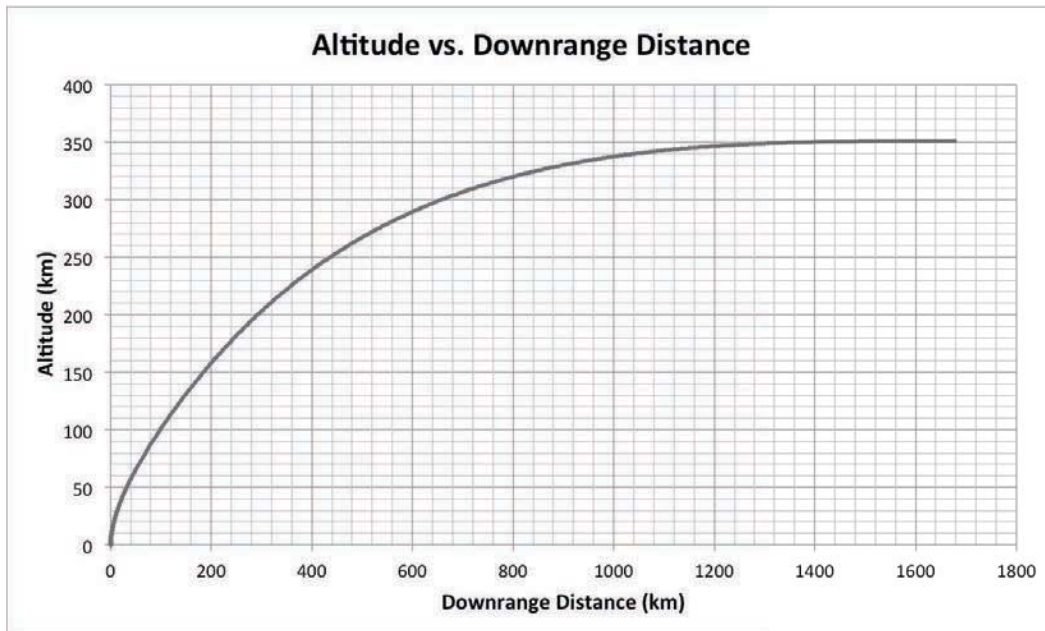


Figure 5. 2D spatial trajectory results.

3.5. Optimal Trajectory Analysis

In practice, trajectories are simulated by utilizing multiple maneuver techniques to achieve the best trajectory for a given cost function (such as minimizing fuel or maximizing final velocity). Launch trajectory optimization involves obtaining the LV dynamic states and controls that optimize the chosen performance index while satisfying imposed trajectory constraints⁸. End conditions (orbital parameters) are specified and the optimization problem is deconstructed into predetermined launch phases that are linked together to avoid discontinuities in the trajectory (no coast periods are involved).

Multiple trajectory optimization software programs exist for analyzing these trajectories. GPOPS (General Pseudospectral OPTimal control Software)—a 3-DOF, MATLAB-based, open-source program that uses *hp*-adaptive pseudospectral methods to solve multiple-phase optimal control problems—was utilized to solve this ascension problem¹¹. The “Multiple-Stage Launch Vehicle Ascent Example” from GPOPS was modified from a two-stage vehicle with nine strap-on solid rocket boosters to the currently investigated vehicle.

The GPOP dynamic model uses the equations of motion for a non-lifting point mass ascending over a spherical rotating planet in Cartesian Earth-centered inertial (ECI) coordinates:

$$\dot{\mathbf{r}} = \mathbf{v} \quad (11)$$

$$\dot{\mathbf{v}} = -\frac{\mu}{\|\mathbf{r}\|^3} \mathbf{r} + \frac{T}{m} \mathbf{u} + \frac{\mathbf{D}}{m} \quad (12)$$

$$\dot{m} = -\frac{T}{g_0 I_{sp}} \quad (13)$$

Boundary constraints include initial position and velocity conditions based on launch site and gross liftoff mass. End constraints were defined by orbital elements (see Table 4) that describe the payload’s final expected location in orbit. The program implemented two path constraints: one to keep the vehicle’s altitude above the surface of the Earth and another to guarantee the control vector (thrust direction) magnitude remains at unit length. Lastly, linkage conditions set constraints to force state variables to remain continuous during phase changes and account for mass ejections. The optimal control problem is then to determine the control that minimizes the cost function:

$$J = -m^{(3)} t_f \quad (14)$$

Where the superscript (3) represents the third (final) phase, and t_f represents the final time at the end of flight.

Table 4. End-of-flight orbital parameter constraints.

Orbital Parameter	Value
a_f (km)	6,748
e_f	0.004
i_f (deg)	51.6
Ω_f (deg)	206.4
ω_f (deg)	103
v_f (deg)	unconstrained

The stage masses and thrust-to-weight ratios obtained from the gravity-turn trajectory analysis were used as initial inputs for the optimal control trajectory problem. A number of test cases were executed with variable parameters changed until a final satisfactory solution was obtained. Figure 6 displays time histories of the altitude, velocity, mass, and control performance parameters, and Figure 7 shows the 2D spatial trajectory of altitude vs. downrange distance.

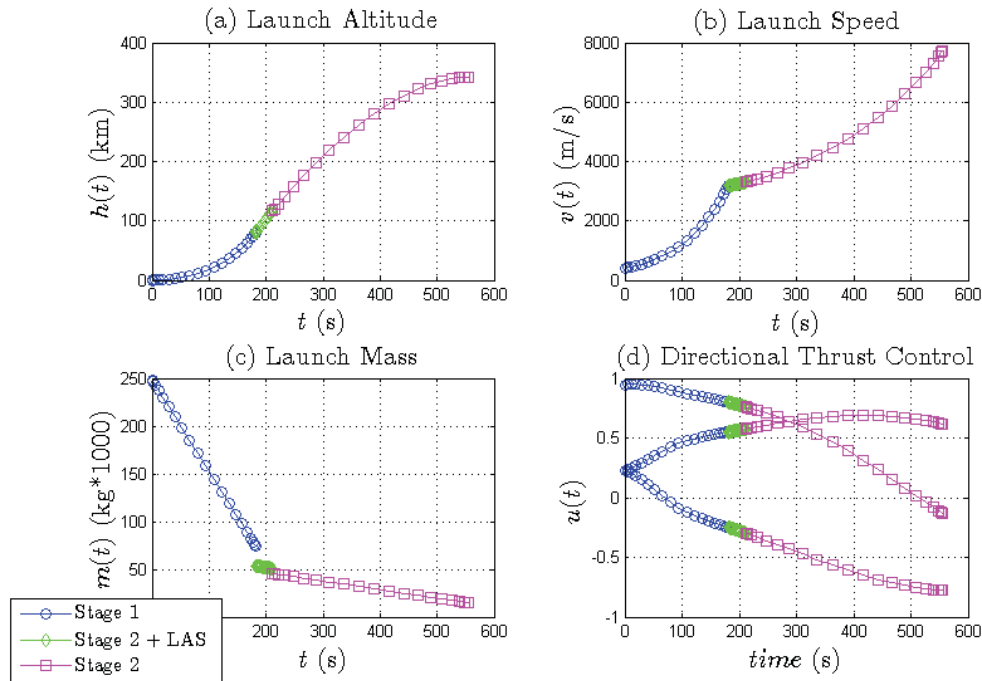


Figure 6. Time histories of (a) launch altitude, (b) launch speed, (c) launch mass, and (d) directional thrust control.

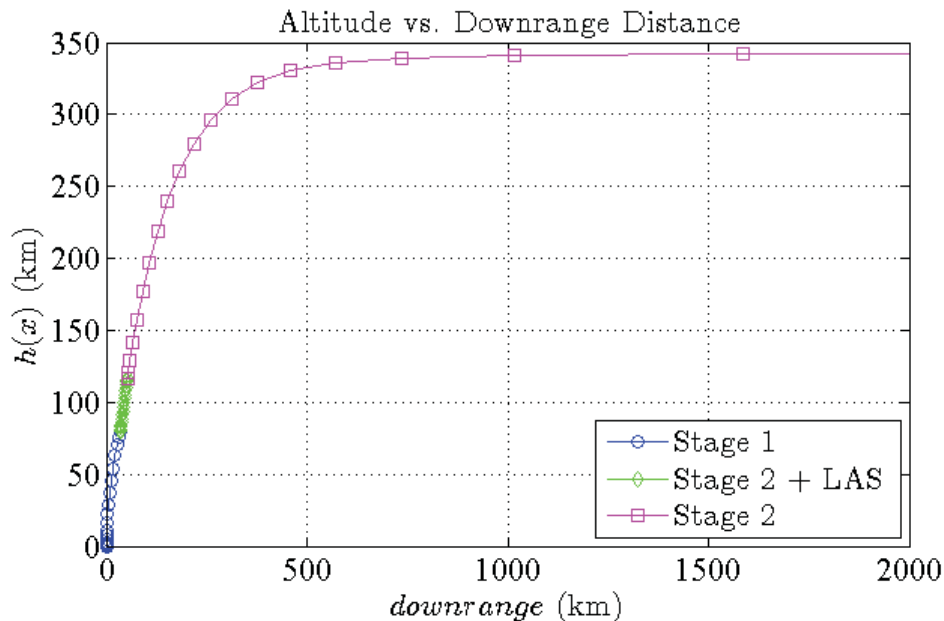


Figure 7. 2D spatial trajectory results.

These results are not completely satisfactory because dynamic loading of the vehicle during max- q (maximum dynamic pressure) and maximum acceleration need to be considered for structural and human factor purposes. It is recommended that a launch vehicle experience only a few hundred pounds per square foot (psf) of dynamic loading, whereas the calculated results are around 1,100 psf during max- q . Human-rated missions strive to keep the peak acceleration at or below 3 g for safety purposes, but results indicate a peak acceleration of about 3.57 g. These issues are typically resolved by allowing the thrust to vary and throttling back before reaching max- q . Unfortunately, the GPOPS code does not enable thrust variation. Future work will include the use of more complex optimization programs, such as OTIS¹² (Optimal Trajectories by Implicit Simulation), which enable more constraint flexibility and parameter variations (including thrust).

3.6. Final Launch Vehicle Design

Figure 8 summarizes the final launch vehicle design[§].

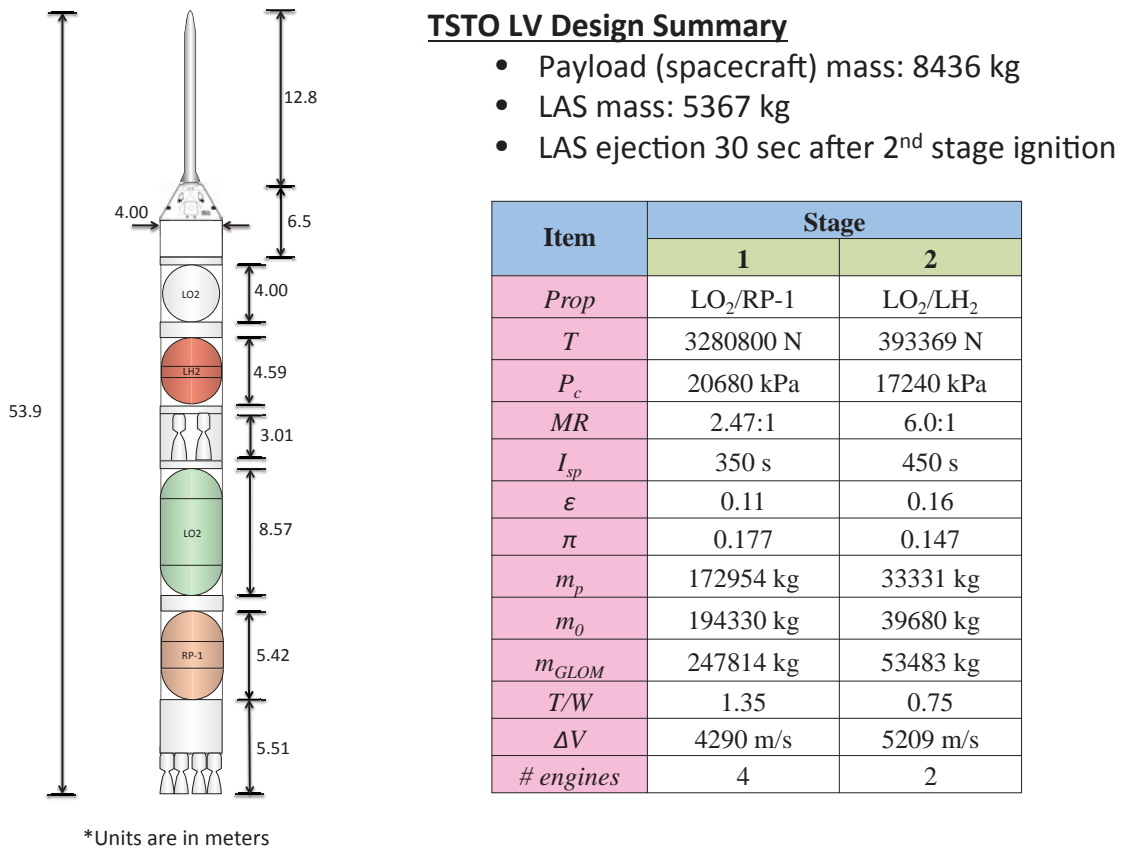


Figure 8. Final launch vehicle design summary.

[§] Sketch was created with INTROS⁷

4. Concept of Operations

Figure 9 depicts the mission concept of operations. During ascent, the first stage separates after about 180 seconds of burn time, followed by LAS jettison 30 seconds after second-stage ignition, and finally second-stage separation and orbit insertion after about 380 seconds of second-stage burn time. Under nominal conditions, the spacecraft orbits Earth for 24 hours and makes any orbital corrections needed to rendezvous and dock with the space station. The spacecraft remains docked for approximately six months, with routine one-hour checkouts every week. Once undocked, the spacecraft prepares for re-entry by performing orbital maneuvers and a “cold soak” to reject any heat accumulated during the docked period. The spacecraft then initiates a deorbit burn with the main engine to reach the entry interface altitude. The service module is jettisoned after the burn and the spacecraft prepares to ballistically re-enter the atmosphere. As the spacecraft begins its approach for landing, the parafoil deploys and can be steered towards a safe ocean splash zone or ground landing area.

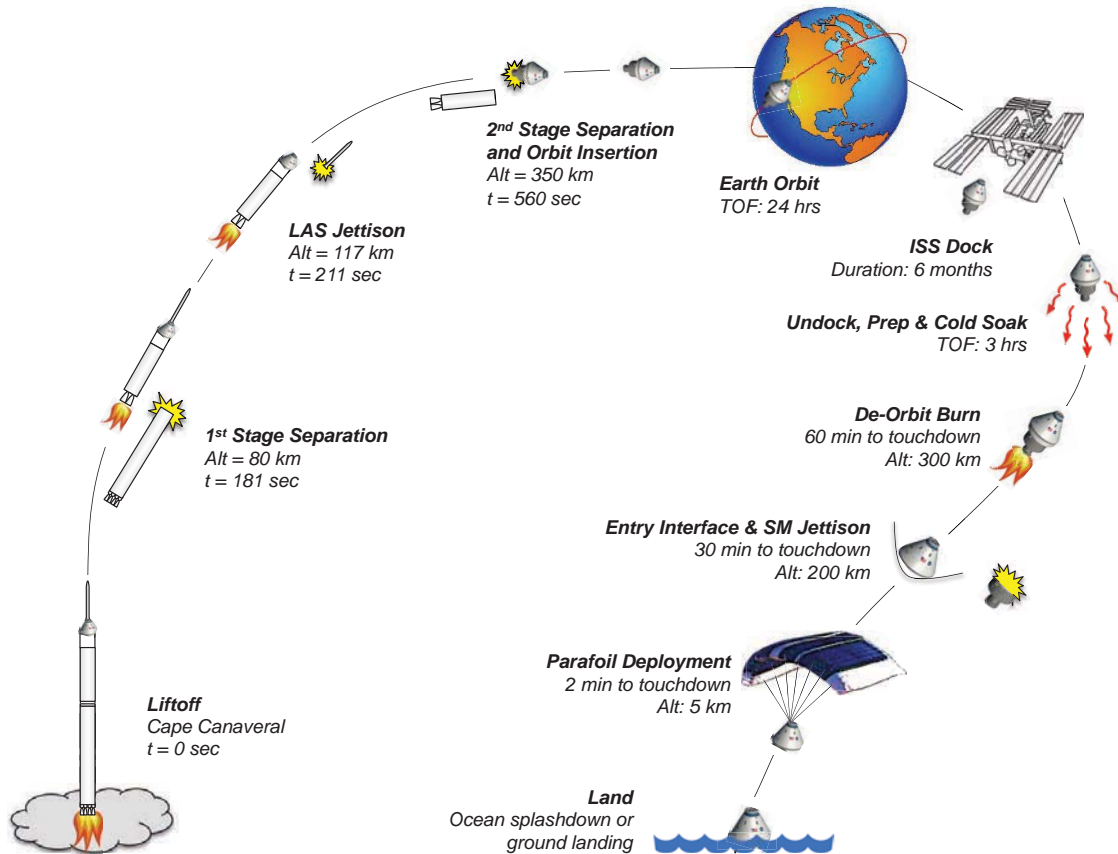


Figure 9. Concept of operations.

5. Spacecraft Subsystems Layout

After approximating the mass for each spacecraft subsystem, a more detailed analysis is performed to generate a subsystem mass equipment list, determine if the total subsystem mass is within the pre-allocated mass envelope, and ensure closure of these subsystems. Each subsystem is designed to the component level for identifying major risks to the mission and crew and aiding in reliability estimates. Most of the subsystem designs are based on procedures outlined in *Human Spaceflight*⁴ unless otherwise noted.

5.1. Structures and Mechanisms

The structures subsystem is essential to the integrity of the pressurized crew compartment and protects the crew from various loads during the mission. It is often divided into three categories: primary (backbone), secondary (appendages), and tertiary (small) structures. The first two categories are the most challenging and influential in the design. Since structures have been historically reliable in human-rated space missions, a detailed mission loads analysis is not necessary for selecting the material and estimating the capsule mass. An exact architectural layout is beyond the scope of this project.

Since welding is the most reliable method to seal a pressurized structure, composites and sandwich construction will not be used for the spacecraft shell. Steel will also not be used since it is susceptible to instability under compressive loads. Aluminum alloys are easily welded and capable of surviving extreme temperatures in space. Aluminum 6061-T6 in particular is less expensive and more readily available than some of its other aluminum alloy counterparts. Allowable tensile-ultimate and compressive-yield stresses for this material are, respectively, 160 MPa and 100 MPa with high-grade machine welds (290 MPa and 240 MPa without welds), and safety factors for ultimate and yield conditions are 2 and 1.5, respectively.

The maximum internal pressure for the crew module design in space is 0.1096 MPa (slightly more than one atmosphere), so the design ultimate internal pressure is twice as much, or 0.219 MPa. Away from the welds, the tensile stress resulting from this pressure cannot exceed the allowable ultimate tensile stress of 290 MPa. The required thickness away from the welds for a capsule with a 2.5 m (2,500 mm) radius is therefore:

$$t_1 = \frac{p_u r}{F_{tu}} = \frac{0.219(2500)}{290} \approx 1.89 \text{ mm} \quad (15)$$

This thickness must be increased about 2 cm from each weld to keep the design yield stress below the welded allowable stress of 100 MPa:

$$t_2 = \frac{p_y r}{F_{ty}} = \frac{1.5(0.1096)(2500)}{100} \approx 4.11 \text{ mm} \quad (16)$$

The ultimate compressive stress needs to be kept less than the elastic buckling stress. For an unpressurized, isotropic, monocoque cylinder (assuming plasticity correction factor of 1.0), the elastic buckling stress is given by:

$$F_{cr} = 0.6\gamma \frac{Et}{r} \quad (17)$$

The ultimate compressive stress, with 1.4 and 1.5 ultimate factors of safety for inertia loads and pressure, respectively, is:

$$f_{cu} = 1.4 \left(\frac{P_c}{2\pi r t} + \frac{M_{max} r}{\pi r^3 t} \right) - 1.5 \frac{pr}{2t} \leq F_{cr} \quad (18)$$

where the peak bending moment, M_{max} , can be estimated from the mass and geometric properties of the capsule as well as the load factors assumed for each phase of flight (taken from those experienced by the Shuttle). The compressive force, P_c , is simply estimated as the capsule weight multiplied by the negative axial load factor.

Assuming the correlation factor, γ , used to match theory with results is 0.5, using the modulus of elasticity for aluminum 6061-T6 (69,000 MPa), and rearranging the inequality to determine the required thickness for stability gives:

$$t_3 = \sqrt{\frac{r}{0.3E} \left[1.4 \left(\frac{P_c}{2\pi r} + \frac{M_{max}}{\pi r^2} \right) - 1.5 \frac{pr}{2} \right]} \quad (19)$$

The capsule thickness results for launch and normal landing flight modes are summarized in Table 5. Taking the larger thickness of 2.13 mm and substituting it in Equation (17) to determine the ultimate compressive stress gives:

$$f_{cu} = 0.3 \frac{Et_3}{r} = 0.3 \left(\frac{69000(2.13)}{2500} \right) \approx 17.6 \text{ MPa} \quad (20)$$

This is well under the material's proportional limit. Since $t_3 > t_1$, the capsule shell is critical for stability and must be at least 2.13 mm thick away from the welds and 4.11 mm thick near the welds.

Table 5. Estimated capsule thickness to prevent buckling under launch and landing loads.

Mission Phase	Limit Load Factors (from Shuttle)			Min. Pressure (MPa)	Limit Compressive Axial Force, P_c (N)	Limit Moment, M_{max} (10^6 mm·N)	Required Thickness, t_3 (mm)
	n_x	n_y	n_z				
Launch	-3.2	1.4	2.5	-0.00345	264,800	104	2.13
Normal Landing	-2.0	1.5	-4.2	-0.00345	165,500	161	1.99

The mass of the primary structure itself is the product of the material density and the volume of the structural module shell. Since the thickness of the capsule varies, the product of the aluminum's area density with the module surface area can be used to estimate the mass. The area density of metallic structures typically ranges from 5 to 15 kg/m², so a conservative density of 10 kg/m² is chosen, which gives a total of 1,021 kg for the primary shell structure (command and service modules).

A launch vehicle adapter (LVA) is needed to connect the LV structure to the spacecraft structure and enable spacecraft separation. LVA mass is a strong function of spacecraft mass, as shown in Figure 10. Using the trend-line equation from this figure, the total estimated mass for the LVA is about 1,092 kg. This is a conservative estimate for the adapter; the LVA for the Orion mission is about 580 kg, which is just a little more than half this mass estimate for a heavier spacecraft. Including hatches, a docking adapter, and smaller items such as tolerances, joints, thermal coatings, etc. (estimated at about 40% of the primary structure), the total mass estimate for the subsystem is about 2,700 kg. Table 6 gives a mass breakdown for the structures and mechanisms subsystem.

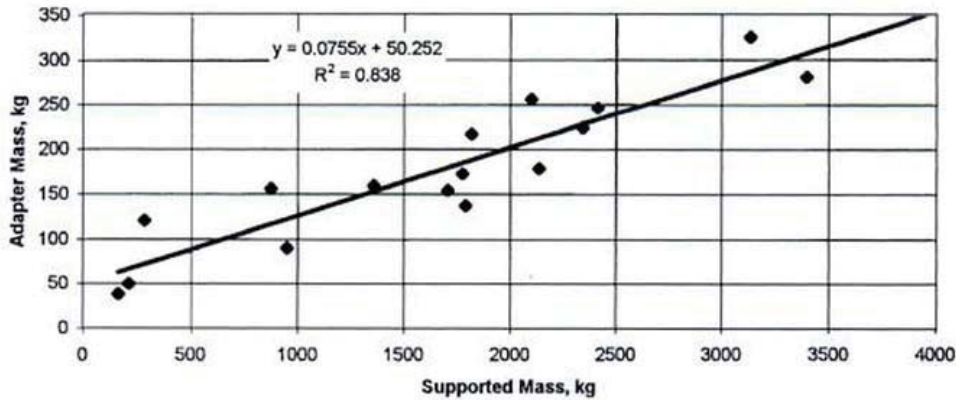


Figure 10. Launch vehicle adapter mass¹³.

Table 6. Structures and mechanisms breakdown.

Item	Mass (kg)
Primary Structure	1,021
Hatches (Side and Forward/Docking)	130
CM-SM Umbilical System	5
Docking Adapter	50
Launch Vehicle Adapter	1,092
Tolerances, Joints, Coatings, Etc.	400
TOTAL	2,698

5.2. Thermal Control System

The thermal control system (TCS) maintains normal operating temperatures for subsystems and equipment, as well as comfortable temperatures for the crew. Two types of systems are used: active or passive systems. Crewed spacecraft require higher power levels and temperatures to accommodate human comfort levels, so active controls need to be implemented. The TCS is different from the thermal protection system, which shields the spacecraft from extreme heat sources and sinks.

Sizing the thermal system involves adding all the heat loads aboard the spacecraft. However, the largest contributions to these loads are from electrical equipment. Therefore, at this stage it is adequate to assume that the total heat load for thermal control is equal to the capacity of the electrical power system, which was previously estimated to be 3 kW. Adding a margin of 20%, the required total heat load for thermal control is assumed to be 3.6 kW.

Thermal control systems consist of three primary elements: heat acquisition, transport, and rejection. The heat acquisition subsystem collects heat from a component via heat-transferring devices (such as a cold plate). The heat transport subsystem carries heat from the acquisition subsystem to be dissipated. The heat rejection subsystem expels excess heat into deep space by radiation or dissipates it with short-duration heat sinks. The decision to use heat sinks or radiators depends on the mission duration. Heat sinks are typically used for extremely short durations (3 days or less for near-Earth orbits), while radiators are typically used for longer durations. For this design, heat sinks will be used during pre-launch and post-landing phases and radiators will be used during on-orbit operations. In addition, refrigerants such as ammonia boilers will be used to handle re-entry loads.

Another element of thermal control is heat generation, which consists of heaters that are used to heat subsystems during the docking period. Heat acquisition subsystems consist of heat exchangers and cold plates, and heat transport subsystems include pumps (with accumulator), plumbing/valves, instruments and controls, and liquid coolant. A fixed-surface radiator was selected for on-orbit heat rejection and its mass can be estimated as 5.3 kg/m² for a two-sided panel. The approximate mass of an expendable heat sink (M_e) is a function of the required heat-rejection rate, mission duration, and latent heat of vaporization (a fluid property):

$$M_e = QD/h_{fg} \quad (21)$$

During pre-launch operations for the Shuttle, up to 250 watts of power were available to perform payload checkouts¹⁴. This power requirement will be used for pre-launch and post-landing heat rejection rates. An ammonia boiler similar to that used by the Shuttle will be used during re-entry. The mass of the Shuttle's ammonia boiler system is about 72 kg (including 44 kg of ammonia) to reject up to 33 kW of thermal energy briefly before, during, and after landing. This mass estimate will be conservative for the spacecraft described here considering the relatively low heat rejection loads experienced during this flight phase.

Passive thermal control will consist of multi-layer insulation (MLI), which contains many thin reflective layers separated by vacuum to help protect the capsule from solar heating and reduce heat loss through thermal radiation. Advanced Flexible Reusable Surface Insulation (AFRSI) blankets¹⁵ used on the Shuttle are considered here to estimate the mass of the MLI, although the technology itself may be outdated and a new, more effective insulation blanket could possibly be used.

Table 7 summarizes the mass, power, and volume requirements for the thermal control hardware, which are stored in the command module. Hardware is sized using MER values based on capacity (per kW of heat transfer) or surface area size. Redundancies are included for heat acquisition and heat transport subsystems to achieve a reliable thermal control system. The total mass is about 600 kg.

Table 7. Thermal control system requirements.

	Item	Mass (kg)	Power (W)	Volume (m ³)
Hardware for Active Thermal Control				
<i>Heat Generation</i>	Heaters (3 redundant)	4	50	-
<i>Heat Acquisition</i>	Heat Exchanger Pair (2 redundant sets)	3.9	0	0.0001
	Coldplates (3 x 1 kW, with redundant set)	72	0	0.168
<i>Heat Transport</i>	Pumps with Accumulator (with redundant set)	34.56	82.8	0.1224
	Redundant Plumbing & Valves	31.97	negligible	-
	Instruments & Control	17.98	negligible	negligible
	Fluids	17.98	-	-
<i>Heat Rejection</i>	Radiator (27.5 m ² fixed, 2-sided)	145.6	negligible	0.55
	Heat Sinks	2.16	negligible	-
	Ammonia Boiler	72	negligible	-
Hardware for Passive Thermal Control				
	Multi-Layer Insulation	200	0	0.7427
TOTAL		602	132.8	1.58

A schematic of the TCS is shown in Figure 11. Two loops are included for redundancy: the primary (inner) loop and the secondary (outer) loop.

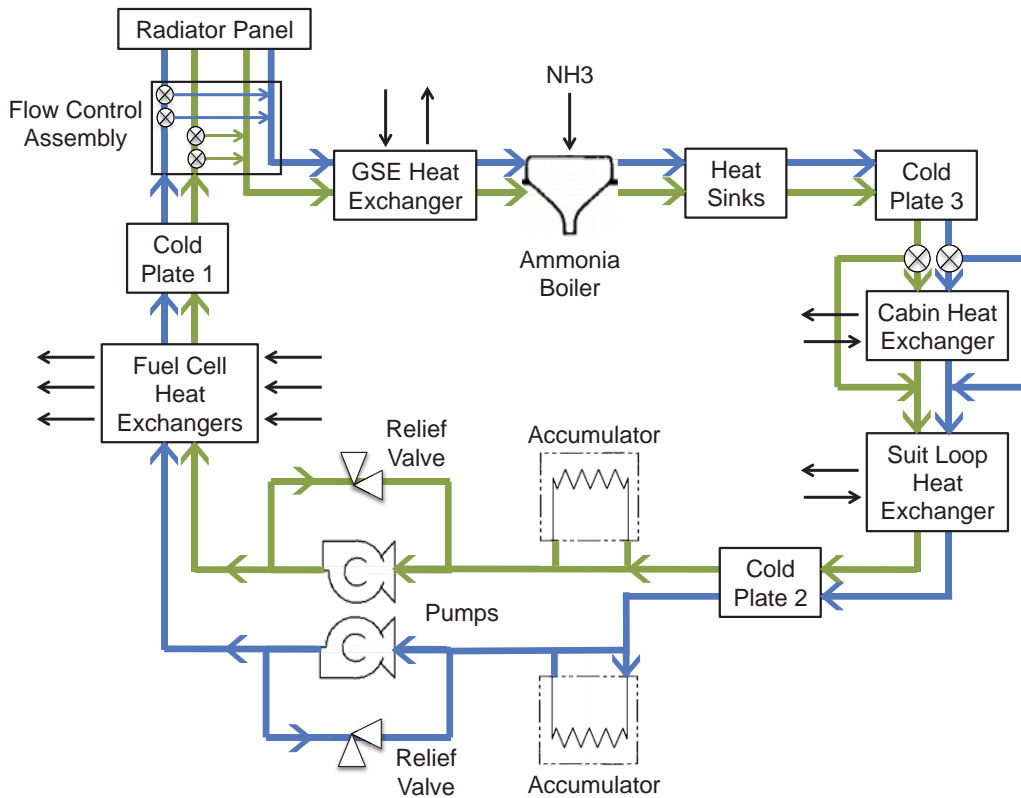


Figure 11. TCS schematic.

NASA has recently been developing an advanced TCS technology concept called the Sublimator Driven Coldplate¹⁶ (SDC), which combines all three TCS functions into a single piece of hardware. This novel concept has the potential to replace an entire thermal control system with just one hardware component that does not consume any power or contain moving parts. This type of TCS is ideal for low heat loads and short mission durations, which could make it useful for this application. Future work may update the generic spacecraft design to consider this technology.

5.3. Environmental Control and Life Support System (ECLSS)

Although all spacecraft subsystems are vital for a successful mission, only the ECLSS exists to keep the crew alive and comfortable. Primary ECLSS functions typically include atmosphere management (monitoring, revitalization, control, and supply); water and waste management; fire detection/suppression, and food storage/preparation¹⁷. For this vehicle, consumables and other crew accommodations (e.g. supplies, equipment, and other provisions) will be considered as a separate “crew accommodations” subsystem (see section 5.7) and not as part of the ECLSS. Table 8 provides a summary of mass, power, and volume requirements for the ECLSS. The total subsystem mass is around 820 kg.

Table 8. ECLSS requirements.

Item	Mass (kg)	Power (W)	Volume (m ³)
Pressure Control Subsystem (PCS)			
Plumbing (CM)	26.76	-	-
Plumbing (SM)	5.96	-	-
Air Revitalization Subsystem (ARS)			
Stored Tanks (CM)	60.5	0	2.73
Stored Tanks (SM)	151.2	0	6.83
LiOH Cartridges (7)	49	12	0.035
HEPA Filters (2)	17	-	0.053
CCA	30	-	0.1
Atmospheric Monitoring Subsystem (AMS)			
Sensors (CM)	3.52	-	-
Sensors (SM)	1.76	-	-
Mass Spectrometer	2.4	100	0
Temperature and Humidity Control (THC)			
Condensing Heat Exchangers (2)	2	100	0.1
Heaters (2)	4	50	-
Water and Waste Management (WWM)			
Stored Water (CM)	57.4	0	0.056
Stored Water (SM)	71.8	0	0.07
Multifiltration	40	160	0.16
VCD	100.0	120	0.4
Waste Collection	45	45	0.05
Supplies and Contingency Bags	7.9	0	0
Fire Detection and Suppression (FD&S), Suit Loop			
Fire Suppressant System	70	-	-
Smoke/CO Detectors (2)	0.8	-	-
Suit Loop	70	-	-
TOTAL	817.0	587	10.58

The design includes two sets of air generation systems (as shown in Figure 12) and two water storage tanks—one of each for the CM and another for the SM. This saves space in the CM and reduces risk of mission or crew failure if any of the pressurized tanks rupture. All other ECLSS components are stored in the CM. Redundancies are included wherever appropriate and some components, although not critical, are added for completeness.

The atmosphere management subsystem consists of pressure control, air revitalization, atmospheric monitoring, and temperature and humidity control. Air revitalization consists of ventilation, make-up gases supply (nitrogen and oxygen), and contaminant removal. Contaminant removal includes controlling and removing carbon dioxide in the atmosphere to keep it from becoming toxic. Early spacecraft designs have used lithium hydroxide (LiOH) canisters to absorb CO₂, but other options include molecular sieves, solid amine water desorption, and electrochemical depolarization concentration. LiOH canisters remove about 2 kg of LiOH daily per each person’s CO₂ output, which cannot be regenerated, making them only ideal for short-duration space missions. Molecular sieves, on the other hand, use synthetic zeolites or alumino-silicated metal, which can be regenerated. The design selects the LiOH canisters because they provide an advantageous mass savings over the sieves for a relatively

short mission. The design also includes a contamination control assembly (CCA) to remove carbon dioxide and acidic gases inside the cabin, along with HEPA filters to effectively remove small particles and bacteria.

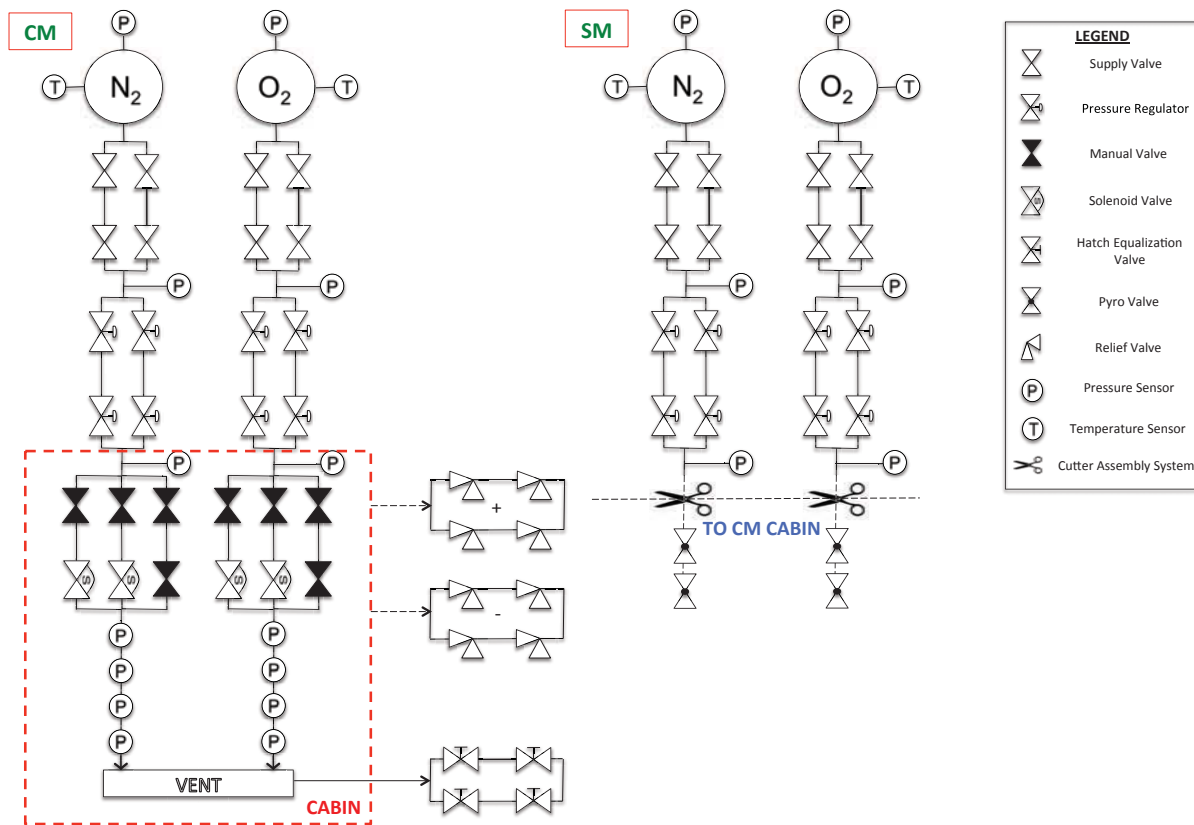


Figure 12. ECLSS air generation system schematic.

Water management consists of storing water, processing water and urine, and distributing water through plumbing, which can be neglected for preliminary design. Water tanks are stored on board and the supply comes from pre-stored water, fuel cell byproducts (see Power section 5.4 for details), and humidity condensate. Multifiltration is used for processing water and vapor compression distillation (VCD) is used to collect and process urine. Waste management consists of a waste collection system and associated supplies.

The fire detection and suppression (FD&S) subsystem typically consists of smoke detectors, alarms and shutoff systems, portable fire extinguishers, gas masks, and oxygen bottles¹⁸.

5.4. Power

Power system options vary depending on mission duration and amount of power required. Batteries are very effective power sources for unmanned spacecraft but are not feasible for manned spacecraft missions that last at least a few days and require several kilowatts of power. Solar cells are ideal for lengthy missions (weeks to years) and orbiting stations, but they require complicated deployment mechanisms and are not ideal for shorter missions. Nuclear reactors can be massive and hazardous to humans, and radioisotope generators tend to be massive and expensive. Regenerative fuel cells are an ideal option for this type of mission and are common powering methods for Earth-orbiting spacecraft missions because they produce high energy per

unit of reaction mass. Hydrogen fuel cells also generate water as a byproduct of electrolysis, and that can be circulated back into the ECLSS for use. The primary disadvantage of fuel cells is the requirement for storing hydrogen and oxygen, but the overall system mass would still be less compared to a battery-powered system.

Power estimates from each subsystem were used to approximate the total baseline and peak power required for the mission. Peak power was determined by taking the highest power requirement value from the crew accommodations subsystem since its components operate for only a small fraction of the mission duration. These estimated power requirements match closely to initial estimates. Therefore, the same power requirements (with margin) are assumed.

Since no MER or power-rating relationship exists for estimating the mass and power supply of a fuel cell, these specifications were taken from a specific fuel cell manufacturer. The parameters shown in Table 9 were calculated from the manufacturer’s 10.5 kW fuel cell datasheet¹⁹ for a 7-day contingency mission. Hydrogen and oxygen are the reactants and water is the emission to be circulated to the ECLSS. The fuel cell efficiency for this specific model is around 51-69% and the durability/lifetime target is about 10,000 hours²⁰.

Table 9. Fuel cell parameters for a 7-day mission duration.

Parameter	Hydrogen	Oxygen	Water
Mass (kg)	2.966	47.05	16.92
Mass Flow Rate (kg/hr)	0.0141	0.112	0.101
Tank Volume (m ³)	0.367	0.367	-
Tank Diameter (m)	0.888	0.888	-
Tank Thickness (mm)	6.44	6.44	-
Tank Mass (kg)	289	289	-
Total Mass (kg)	291.97	336.05	16.92

Power management and distribution components are also considered in the power subsystem design. These include the regulators, converters, charge controllers, and wiring required to connect the power sources and deliver the appropriate voltage-current levels to all power subsystems and loads while enabling the system’s degradation during the mission. Figure 13 displays a generic power system block diagram with fault protection for the power management system.

The electrical power system can be decomposed into three categories: generation, distribution, and storage. Power generation consists of the fuel cell stacks, heaters and heat exchangers, and plumbing (pressure regulator and sensor, purge valve, and water separator) used to generate the power and control flow from the reactant gases. Distribution involves the cabling, coolant, bus, and power control units. The storage involves the reactant gases and water output. Two additional fuel cell, heater, and heat exchanger hot spares are included for redundancy. The mass of the power distribution system is estimated as 6% of the initial spacecraft mass. Table 10 gives a breakdown of the fuel cell system masses. The total mass of the power system is about 1,030 kg.

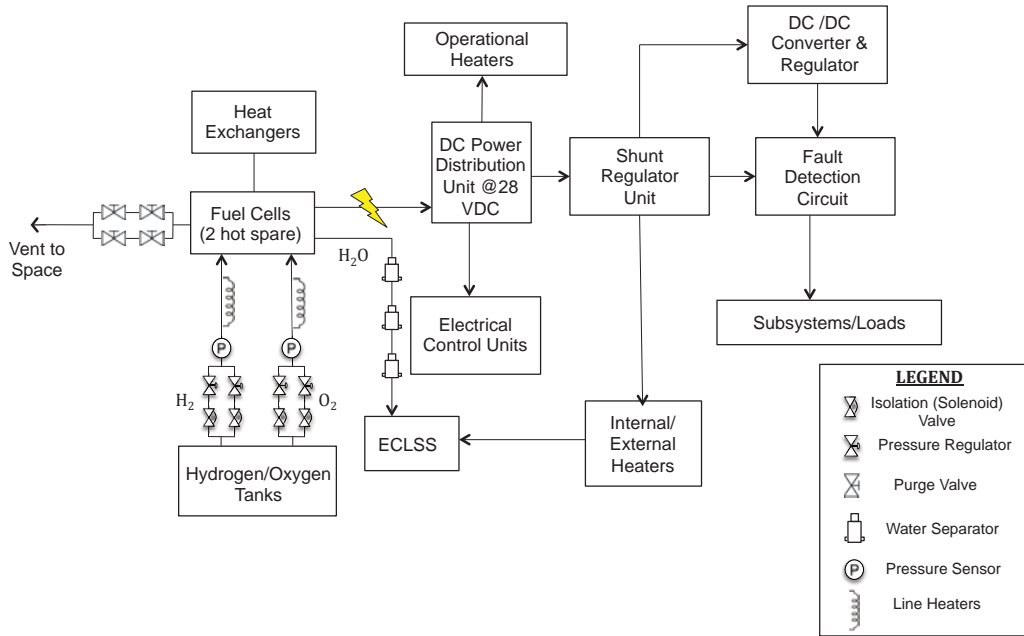


Figure 13. Generic power system block diagram.

Table 10. Fuel cell system mass breakdown.

Item	Mass (kg)	Volume (m ³)
Power Generation		
Fuel Cell Stacks (3)	32.1	0.048
Heaters (6)	6	-
Heat Exchangers (3)	1.95	-
Plumbing	6.88	-
Power Distribution		
Cabling, Coolant, etc.	340	-
Power Storage		
Hydrogen Tank	292	0.367
Oxygen Tank	336	0.367
Water Output	16.9	0.017
TOTAL	1,032	0.80

5.5. Avionics

Avionics are the electronics used on a spacecraft and typically include guidance, navigation, and control (GNC); tracking/communications; command and data handling; and crew interface. Most avionics items were selected from examples of currently available components since electronics continue to rapidly improve, resulting in weight, power, and volume savings. A few components were selected from the Shuttle orbiter and assigned a “Shuttle technology factor” to compensate for technological advances.

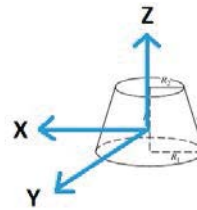
GNC is the integrated field that studies the combination of sensors, actuators, and algorithms to control the vehicle’s attitude and apply the necessary torques to re-orient it to a desired state. It is mainly responsible for stabilizing the space vehicle when disturbance torques are encountered. For low-Earth orbiting spacecraft, the primary disturbances encountered are atmospheric drag and gravity-gradient torques. For this specific mission, where no interplanetary transfers or plane changes occur, GNC is only used for orbital correction maneuvers and re-entry control.

Table 11 shows: (a) assumptions made to calculate space environment disturbances and (b) the resulting disturbance torques. The center of mass and moments of inertia were estimated by considering the capsule as a conical frustum with a small top radius (0.1 m), and the vehicle's center of pressure offset was assumed to be 5% of the largest diameter¹³. Assumptions about each disturbance were made (e.g., field strengths and incidence angles) to yield a rough order-of-magnitude estimate of disturbances^{**}.

Table 11. (a) Estimated spacecraft parameters (left), and (b) resulting disturbance torques (right).

Parameter	Value	Units
h	350	km
R_E	6,378	km
μ_E	3.986E+14	m^3/s^2
$d_{largest}$	4	m
$cp_s - cm$ (5%)	0.2	m
d_{mean}	2	m
cm	1.212	m
I_x	19,368	$kg\cdot m^2$
I_y	19,368	$kg\cdot m^2$
I_z	26,404	$kg\cdot m^2$

Disturbance	Torque (N-m)
Solar	9.2E-06
Atmospheric	2.9E-02
Gravity-Gradient	2.4E-03
Magnetic Field	4.0E-05



Two types of stabilization and control techniques exist: passive and active stabilization. Passive control techniques include gravity-gradient stabilization, where the vehicle's inertia is used to keep the spacecraft pointing towards the Earth's center, and spin-stabilization, where the entire spacecraft rotates to keep its angular momentum vector fixed in inertial space. Active stabilization involves the use of attitude sensors, attitude actuators, and typically a processor. The sensors take measurements to compute the spacecraft's angular position/velocity and the actuators depend on an implemented control law to counter disturbance torques²².

Passively controlled stabilization systems yield very low attitude accuracies, and since human safety is imperative, pointing accuracies must be high. A common, three-axis active stabilization system is therefore used for GNC. Typical sensors include an inertial measurement unit (IMU), which consists of gyroscopes, accelerometers, and sometimes magnetometers; sun sensors or star trackers; and GPS or an inertial navigation system (used for both altitude and range determination).

The command and data handling (C&DH) subsystem is essentially the "brains" of the spacecraft and has primary control over all functions and operations. Key components include flight computers, software, and data buses. The crew interface subsystem consists of all hardware that the crew uses to interact with the spacecraft, including keyboards, monitors, hand controllers, and display units. Finally, the communications and tracking subsystem provides two-way communication between crew and mission control. Antennas, transponders, and supporting equipment comprise this subsystem. Table 12 provides the breakdown of all avionics equipment required for these subsystems. Redundancies are included where appropriate. The total mass for the avionics system is about 400 kg.

^{**} Calculations were made from equations in *Brown*¹³ and *SMAD*²¹

Table 12. Avionics components mass breakdown²³⁻²⁹.

Item	Manufacturer	Mass (kg)	Power (W)	Volume (m ³)
Guidance, Navigation, Control				
Sensor Monitor	Unknown	10	55	-
Integrated GPS/INS (3)	Honeywell	28.5	45	0.016
Star Tracker Package (2)	Ball Aerospace	12	16	0.01
VNS Lidar	Ball Aerospace	12	60	0.018
Command and Data Handling				
Vehicle Management Computers (4)	Honeywell	60	900	0.05
VMC ISS Interface Cards (4)	Generic	0.4	0	0
Mass Memory Units (4)	Unknown	10	50	0.02
Multiplexers/Demultiplexers (19)	Honeywell	152	532	0.19
Data Bus Isolation Amplifiers (4)	Singer Electronics Systems Division	6.8	0	0.003
Data Buses (4)	Unknown	28	0	-
Crew Interface				
Remote Interface Units (2)	ACE	1.8	30	0.002
Keyboards (2)	Generic	1.8	0	0.0048
Monitors (2)	Generic	8	0	0.01
Hand Controllers (2 rotational, 2 translational)	Generic	8	0	0.002
Head-Up Displays (2)	SAAB	24	35	-
Communications and Tracking				
Integrated S-Band Transponders (2)	Thales Alenia Space	5.2	30	0.015
Filters/Switch Dplexers	Generic	2	-	-
Power Amplifiers (2)	Generic	9	0	0
Low-Noise Filter	Generic	0.1	0	0
S-Band Parabolic Antennas (2)	Generic	18	100	0.2
Switching Mechanism Parts (2)	Generic	0.2	0	0
TOTAL		398	1853	0.54

5.6. Propulsion

The propulsion system connects the propellants to both the thrusters and the main engine, and consists of the fuel and oxidizer (and their tanks); pressurant; hardware components such as valves, filters, and transducers; mounting hardware, insulation, and plumbing; and a hydraulic thrust vectoring control system (TVCS)¹³. MMH and NTO were already selected for the fuel and oxidizer, respectively, and helium was selected as the pressurant. MERs were used to size tanks for all three consumables.

The system can be subdivided into two categories: the main propulsion system (MPS) and reaction control system (RCS). The latter includes the bi-propellant thrusters used for attitude control, and the former covers everything else. The main engine performs the deorbit burn while the thrusters are used for orbital corrections and re-entry orientation. Typically, 12 thrusters are needed for full three-axis control—four for each of the roll, pitch, and yaw maneuvers¹⁷ (two in each direction). This design includes 24 thrusters: 12 on the CM and 12 on the SM. The CM thrusters serve as diverse backups to the SM thrusters during orbital maneuvers, and only 6 thrusters are needed for re-entry. This enables a fully redundant RCS.

A generic propulsion-RCS schematic for this spacecraft is shown in Figure 14. The propellant feed lines are connected to the main engine and the 24 thrusters. Table 13 summarizes the masses for all items in the propulsion system. The total mass of the system is about 860 kg.

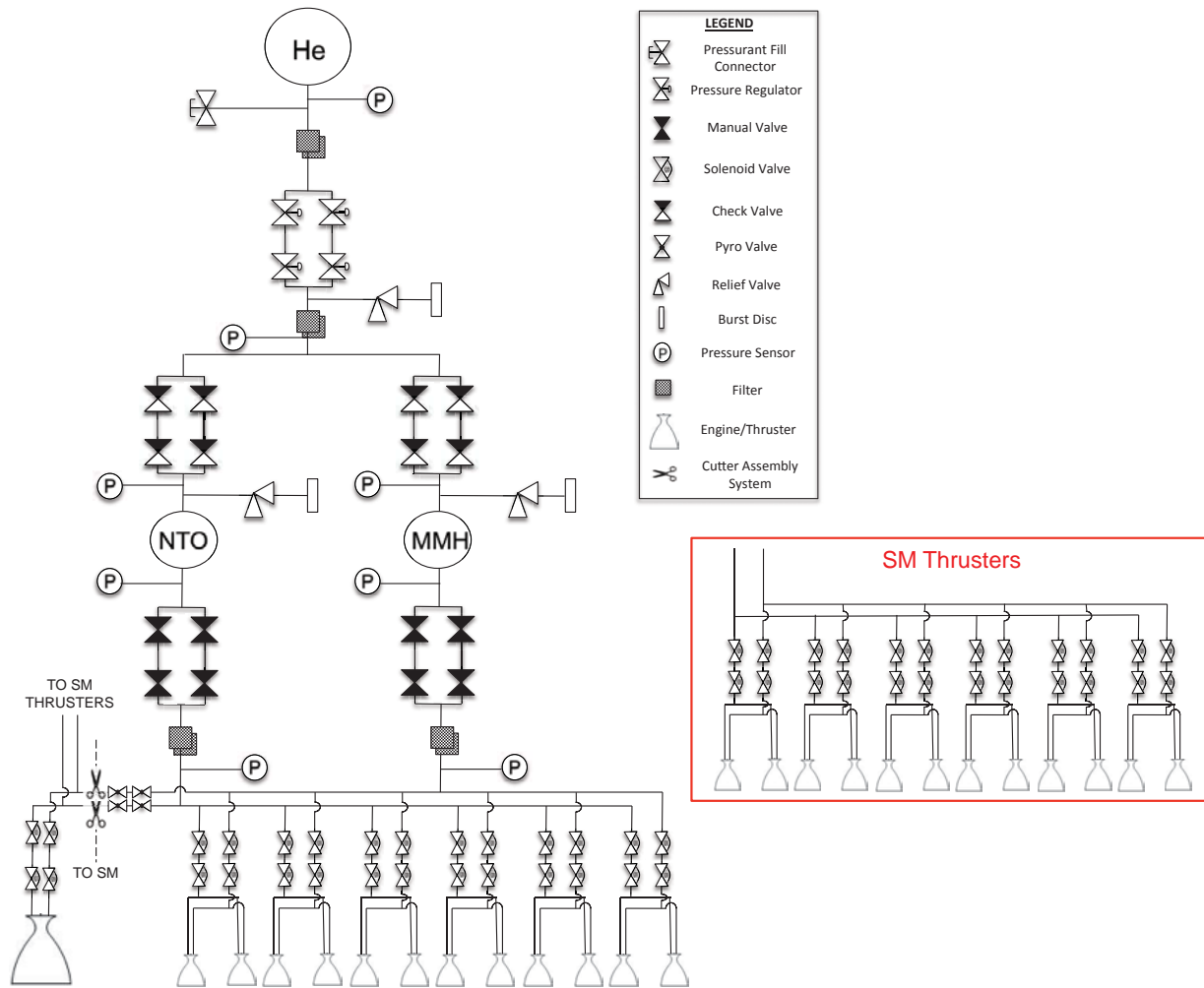


Figure 14. Propulsion-ADCS schematic.

Table 13. Propulsion system mass breakdown.

Item	Mass (kg)	Volume (m ³)
Main Propulsion System		
Main Engine	100	-
Hydraulic TVCS	150	-
Fuel Tank	176.3	0.167
Oxidizer Tank	245.8	0.167
Pressurant	27.3	0.036
Plumbing (Valves, Filters, etc.)	43.35	-
Mounting Hardware, Insulation, etc.	70	-
Reaction Control System		
Bi-Propellant Thrusters (24)	48	-
TOTAL	861	0.37

5.7. Crew Accommodations

Crew accommodations are the elements and procedures that most directly serve human needs, such as food, clothing, hygiene and housekeeping supplies, workstations, maintenance hardware, sleep and recreational equipment, and others. The mass, power, and volume required for these accommodations are strongly dependent on the number of crewmembers and mission duration (often as a function of persons, days, or both). For the short-duration mission presented here, accommodations are kept to a minimum and many noncritical resources are excluded. As previously mentioned, most of the accommodations are powered for only a fraction of the day (at most 8%), so the total power required is just the maximum power among all items. Table 14 provides a summary of the necessary crew accommodations. Including space suits, the total mass is around 640 kg.

Table 14. Crew accommodations mass breakdown.

Item	Description	Mass (kg)	Power (W)	Volume (m ³)
Galley and Food Systems	Food/warmer, kitchen/oven cleaning supplies, sink/spigot, cooking/eating supplies	74.15	0	0.286
Personal Hygiene	Handwash/mouthwash faucet, personal hygiene kit, supplies	17.3	0	0.072
Clothing	Clothes	18.4	0	0.128
Recreational Equipment	Personal storage / closet space	40	700	0.020
Housekeeping	Vacuum (prime + 2 spares), disposable wipes, trash bags	18.6	400	0.315
Operational Supplies and Restraints	Supplies, restraints, and mobility aids	65	0	3.379
Maintenance	Hand tools/accessories, test equipment, fixtures, machine tools, gloveboxes, etc.	125	2,000	0.49
Photography and Film	Equipment	50	400	0
Sleep Accommodations	Sleep provisions (bags/beds, restraints, or rigid stations)	18	0	0.2
Health Care	Medical/surgical/dental suite	15	1,500	0.25
Space Suits	Suits for crew (4)	200	0	0.4
TOTAL		641	2,000	5.54

5.8. Entry, Descent, and Landing (EDL)

Atmospheric re-entry is when a spacecraft returns from orbit, encounters the planet's atmosphere, and uses the atmosphere to aerodynamically decelerate and prepare for landing. Space vehicles re-entering from a parking orbit can do so ballistically—that is, without generating any lift—if they are blunt, axisymmetric shapes.

Re-entry heat loads require the spacecraft to have a thermal protection system (TPS) with ablative heat shields to protect the capsule. PICA-X, a reusable and less expensive modification of the PICA (Phenolic Impregnated Carbon Ablator) TPS material, was selected for the spacecraft. PICA is a modern TPS material, developed at NASA ARC, with low density and efficient ablative capability at high heat flux. PICA-X, developed more recently by NASA ARC and Space Exploration Technologies Corporation (SpaceX), is an improved TPS technology that is easier to manufacture³⁰. TPS mass is estimated by using the material's density and thickness over the spacecraft's exposed surface area.

After initial re-entry, descent can be controlled through the use of parachutes or parafoils, and landing for a blunt capsule involves an ocean splashdown or ground area touchdown. Parafoils were chosen for this spacecraft design because they deploy like parachutes but can glide and steer toward a landing target. The parafoil system’s mass is a function of its sink rate and the vehicle mass. Typical spacecraft sink rates for parafoils are near 7.5 m/s, so this value is assumed. For the vehicle mass and assumed sink rate, a parafoil system with a lift-to-drag ratio of 3.0 and a density of 1.197 kg/m² will have a mass of approximately 300 kg. Lower sink rates or higher lift-to-drag ratios yield more massive parafoil systems.

Table 15 summarizes approximate masses and volumes for both the TPS and parafoils. A backup parafoil is included in the design for redundancy since parachutes and parafoils are susceptible to getting tangled and can have deployment issues. The total mass is about 1,020 kg.

Table 15. EDL mass and volume estimations.

Item	Mass (kg)	Volume (m ³)
Parafoils (x2)	600	7.784
TPS (PICA-X)	424	1.5708
TOTAL	1,024	9.355

5.9. Spacecraft Subsystem Summary

The updated mass budget is presented in Table 16. Some items were shifted/rearranged or combined into other subsystems. The total mass is estimated to be 13,800 kg, which is a difference of about 0.02% from the initial estimated mass budget.

Table 16. Updated mass budget.

Subsystem	% Mass	Mass (kg)
Structure & Mechanisms	20	2,698
Thermal Control	4	602
ECLSS	6	817
Power	7	1,032
Avionics	3	398
Propulsion	6	861
Crew Accommodations	5	641
EDL	7	1,024
Launch Abort System	39	5,367
Payload (Crew)	3	360
GROSS MASS	100	13,800

6. Safety Design and Risk Analysis

Safety design for spacecraft involves tradeoffs between component mass/volume and redundancy. Risk and reliability analyses employ statistical methods to estimate the reliability of a system in order to mitigate risk. Two approaches to determining the system reliability are fault-tree analysis and subsystem analysis. The former calculates reliability by breaking the mission into multiple phases and identifying different “hazards” or events that can jeopardize the crew’s safety within each phase. For example, the mission can be decomposed into the launch, orbit,

and re-entry phases, with the main event being loss of mission (LOM) or loss of crew (LOC) (Figure 15). Each phase is a contributing event and all are separated by an “OR” logic gate since they are treated as mutually exclusive events. Each of those contributing events would have their own contributing sub-events of major failures that can occur in that mission phase. Probabilistic risk assessment (PRA) is then performed by determining the reliabilities of each subcomponent and working up towards the main event to compute its overall probability.

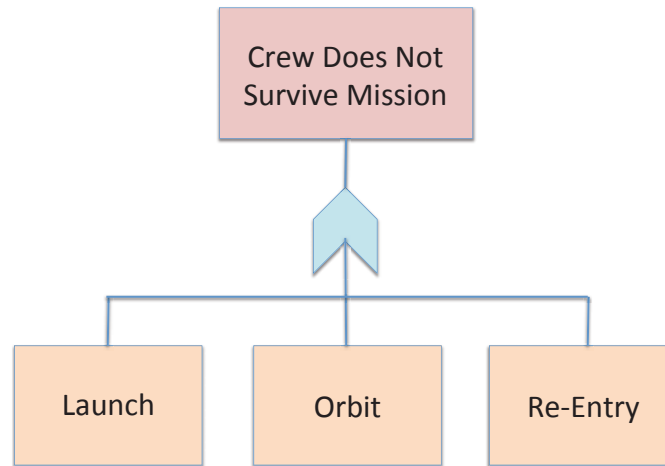


Figure 15. Fault tree of main event.

The subsystem analysis, which is employed here, considers each subsystem separately for all mission phases. The total risk exposure time, as well as the system response to failure (spares, thresholds, etc.), is determined for every assembly and component of a system. The analysis determines each assembly and component’s risk/reliability for the whole mission and then works up to the subsystem reliabilities and, eventually, the system reliability.

6.1. Spacecraft Reliability

Analyzing systems involves using combinations of basic reliability constructs to estimate a unit’s reliability. These constructs apply for units that are in series, in parallel, on standby, or cross-linked. The true reliability of a unit can be estimated by:

$$R(t) = e^{-\lambda t} \tag{22}$$

where t is the operation time and the failure rate, λ , can be inputted directly if a component’s failure rate is given or can be estimated as the inverse of the mean time between failure (MTBF). Most failure rate data were taken from historical databases, the *Aerospace Failure Data Handbook*³¹, or from the manufacturer’s site if a specific component was selected^{19,24-25,32-35}.

The risk exposure times are separated into the different mission phases: ascent, pre-docked, docked (on and off), post-undocked, and EDL. The pre-docked phase is assumed to be the 24-hour mission in orbit, and the docked phase is assumed to be a six-month period where the spacecraft is docked to the ISS. Another assumption is that critical subsystems/components will be turned on once a week for an hour during the docked period for routine checkout (docked on). Also, the post-undocked period involves a cold soak and de-orbit burn until the capsule reaches proper entry conditions. Table 17 shows the risk exposure time breakdown.

Table 17. Risk exposure time for each mission phase.

Mission Phase	Risk Exposure Time (hrs)
Ascent	0.154
Pre-Docking	24
Docked (Off)	4,366
Docked (On)	26
Post-Undock	3.5
EDL	0.5
TOTAL	4,420.15

The system response to failure for each component includes number of cold/hot spares, abort threshold and abort time, LOC threshold, and any LOM/LOC diverse backups (non-identical redundancies) for that component. Hot spares are identical redundant backups that are kept powered for seamless operation transition if the primary component fails, while cold spares are not powered and have to be “switched” following primary component failure. The abort threshold is the number of components that should remain before the mission is aborted; if it is 1, then the mission aborts when one component remains. The abort time is the time it takes the spacecraft to safely land following abort initiation, which could occur at various times throughout the mission. Similar to the abort threshold, the LOC threshold is the number of components that remain to have a loss of crew. For most components, this number is 0, meaning that when all the components of a type fail, the crew will not be expected to survive the mission (worst-case scenario). Some components, however, are not critical to crew survivability and do not have a LOC threshold. Diverse backups are redundant spares that are non-identical to the primary component, meaning they come from different manufacturers and/or use different methods to achieve the same function. These are important because of “common cause” failures, which occur when a single failure mode affects the operation of multiple devices that would otherwise be considered independent (e.g., software, manufacturer defect, or environment).

The mission is designed such that the ECLSS consumables have separate systems for the command and service modules and none of the command module reserves are used prior to undocking. If SM consumables experience a failure, the mission aborts and the crew uses CM reserves to return to Earth.

Additional events and hazards are included in the reliability analysis, such as software failure, rendezvous/docking failure, hatch opening failure, fire, micrometeoroid and orbital debris (MMOD) penetration, bird strike, and space radiation. Table 18 provides a summary of the LOM and LOC risk and reliability results for the spacecraft system. Some components were shifted to other subsystems because of their failure modes (e.g., parafoils moved to ‘mechanisms’), and some components with noncritical failures were not modeled.

The analysis shows that there is a roughly 1 in 52 chance for loss of mission and 1 in 1,038 chance for loss of crew. Redundancies were included in the system (as represented by previous mass breakdowns) to achieve this desired outcome. The TPS was not modeled since that would require thermal analysis that is beyond the scope of this project.

Table 18. LOM and LOC risk and reliability analysis results.

Subsystem	Risk		Reliability	
	LOM	LOC	LOM	LOC
LV Equipment	1.3473E-05	1.3473E-05	9.9999E-01	9.9999E-01
Structure and Mechanisms	8.5076E-04	1.7181E-04	9.9915E-01	9.9983E-01
Power	3.3384E-03	1.0120E-04	9.9666E-01	9.9990E-01
Propulsion	1.5461E-03	3.0901E-04	9.9845E-01	9.9969E-01
Avionics	1.8332E-03	4.2607E-05	9.9817E-01	9.9996E-01
ECLSS	1.0271E-03	6.0440E-05	9.9897E-01	9.9994E-01
TCS	3.1590E-03	5.2389E-05	9.9684E-01	9.9995E-01
Crew Accommodations	1.2387E-04	1.2388E-05	9.9988E-01	9.9999E-01
Events and Hazards	7.5814E-03	2.0049E-04	9.9242E-01	9.9980E-01
TOTAL	1.9327E-02	9.6344E-04	9.8067E-01	9.9904E-01

6.2. Launch Vehicle Reliability

Launch vehicle reliability involves failure modes associated with launch sequence events. These include stage separation failure, re-contact during staging, engine startup failure, loss of control, structural failure, and tank (pressure vessel) failure. Table 19 shows the risk and reliability results for critical LV failure modes.

The analysis shows that there is a roughly 1 in 85 chance for launch vehicle failure. Failure rates for contained/uncontained engine failures were allocated to have the design fit the existing class of launch vehicles. A detailed risk analysis is beyond the scope of this report and the work presented here is not meant to represent a full or competitive risk assessment.

Table 19. LV risk and reliability results^{31,36}.

Stage(s)	Failure Mode	Risk	Reliability
1	Contained Engine Failure	4.00E-03	9.96E-01
1	Loss of Control (engine out + gimbal)	3.24E-04	9.9968E-01
1	Loss of Control (avionics + software)	7.41E-05	9.9993E-01
1	Catastrophic Engine Failure	1.09E-03	9.9891E-01
1	Structural Failure	3.40E-06	1.0000E+00
2	Structural Failure	3.40E-06	1.0000E+00
1	LOX Tank Failure	8.20E-06	9.9999E-01
1	RP Tank Failure	9.70E-06	9.9999E-01
2	LOX Tank Failure	8.20E-06	9.9999E-01
2	LH2 Tank Failure	9.70E-06	9.9999E-01
1,2	Failure to Stage	5.00E-04	9.9950E-01
1,2	Re-contact at Staging	0.00E+00	1.0000E+00
2	Contained Engine Failure	4.50E-03	9.9550E-01
2	Loss of Control (engine out + gimbal)	3.24E-04	9.9968E-01
2	Loss of Control (avionics + software)	7.41E-05	9.9993E-01
2	Uncontained Engine Failure	1.00E-03	9.9900E-01
TOTAL		1.1873E-02	9.8813E-01

7. Summary

This memorandum has presented generic spacecraft and launch vehicle designs developed for a mission delivering four crewmembers and equipment to the ISS. The spacecraft subsystems were designed to the component level for a 24-hour on-orbit mission with a 7-day contingency, and redundancies were implemented to achieve a LOM probability of less than 1 in 50, and a LOC probability of less than 1 in 1,000. A TSTO launch vehicle was iteratively designed to achieve a 350-km orbit by using a combination of MERs and trajectory analyses. Reliability analysis estimates the launch vehicle failure probability to be around 1 in 85. Future work will include higher-fidelity launch trajectory analysis, analysis of launch vehicle loads during flight, and development of a more detailed architectural layout for the spacecraft. The vehicle designs presented are not intended to represent a viable architecture, but rather to provide a non-sensitive, non-proprietary platform for risk analysis studies and development efforts. This generic space launch architecture will be used to perform risk trade studies and to develop, test, and demonstrate innovative Engineering Risk Assessment capabilities at NASA Ames Research Center. These efforts will provide insight into key system risk sensitivities, factors affecting risk analysis estimates, and how to most effectively capture the impactful risk information needed to design safe human spaceflight vehicles.

References

1. "Commercial Crew Program." *NASA Facts*. National Aeronautics and Space Administration, 2011. http://www.nasa.gov/pdf/609181main_12.08.11_CCP.pdf
2. *Man-Systems Integration Standards*. NASA STD-3000. National Aeronautics and Space Administration. Houston, TX: 1995.
3. *Mass Estimating and Forecasting for Aerospace Vehicles*. Systems Definition Branch. National Aeronautics and Space Administration. Houston, TX: 1994.
4. Larson, Wiley J., L. Pranke. *Human Spaceflight – Mission Analysis and Design*, McGraw-Hill, NY: 2000.
5. "Single Impulse De-orbit from Circular and Elliptical Orbits ." *Orbital and Celestial Mechanics*. C. David Eagle, 09 Dec 2012. <http://www.cdeagle.com/pdf/deorbit.pdf>
6. "Space Suit Evolution: From Custom Tailored To Off-The-Rack." *NASA History Program Office*. ILC Dover, Inc.: 1994. <http://history.nasa.gov/spacesuits.pdf>
7. Lynn, Emory E., INTROS User's Manual, 2007.
8. Edberg, Donald. *ARO 409: Introduction to Launch Vehicle Design and Systems Engineering* (class notes). California State Polytechnic University, Pomona. Aerospace Engineering Department. Pomona, CA: 2012.
9. Curtis, Howard D. *Orbital Mechanics for Engineering Students*. 1st ed. Burlington, MA: Elsevier, 2005.
10. "Rocket Mass Characteristics V4.6." *EarthLink*. Earthlink, Inc., 30 Dec 2009. http://home.earthlink.net/~apendrag/atg/coef/Structural_Coef.pdf
11. Rao, A. V., Benson, D. A., Darby, C., Patterson, M. A., Franconin, C., Sanders, I., and Huntington, G. T. 2010. "Algorithm 902: GPOPS, A MATLAB software for solving multiple-phase optimal control problems using the Gauss pseudospectral method." *ACM Transactions on Mathematical Software* 37, 2, 22:1–22:39
12. Riehl, J. P., Paris, S. W., and Sjauw, W. K., "Comparison of Implicit Integration Methods for Solving Aerospace Trajectory Optimization Problems," AIAA 2006-6033, 21-24 Aug. 2006.
13. Brown, Charles D. *Elements of Spacecraft Design*. Reston, VA: American Institute of Aeronautics and Astronautics, 2002.

14. Dumoulin, Jim. "Mission Preparation and Prelaunch Operations." *NSTS 1988 News Reference Manual*. NASA Kennedy Space Center: 1988.
15. Sawko, Paul M., and Howard E. Goldstein. "Performance of uncoated AFRSI blankets during multiple Space Shuttle flights." *NASA STI/Recon Technical Report N 92* (1992): 29104.
16. Stephan, Ryan A. "Overview of NASA's Thermal Control System Development for Exploration Project." *NASA Technical Reports Server*. (2010).
17. Edberg, Donald. *ARO 491L: Introduction to Spacecraft Design* (class notes). California State Polytechnic University, Pomona. Aerospace Engineering Department. Pomona, CA: 2011.
18. "International Space Station: Environmental Control and Life Support System." *Boeing Defense, Space, and Security*. The Boeing Company. <http://www.boeing.com/boeing/defense-space/space/spacestation/systems/eclss.page>
19. "Fuel Cell Products: FC Velocity 9SSL." Ballard. Ballard Power Systems, Inc.: 2011. <http://www.ballard.com/fuel-cell-products/fc-velocity-9ssl.aspx>
20. "PEM Fuel Cell Product Portfolio." *Ballard*. Ballard Power Systems, Inc.: 2011.
21. Wertz, James R., David F. Everett, and Jeffrey J. Puschell (Editors). *Space Mission Engineering: The New SMAD*. Hawthorne, CA: Microcosm, Inc., 2011.
22. de Ruiter, Anton H., Christopher Damaren, and James R. Forbes. *Spacecraft Dynamics and Control: An Introduction*. West Sussex, UK: John Wiley & Sons, Ltd., 2013.
23. Petty, John I.. "HSF - The Shuttle." *Human Spaceflight*. National Aeronautics and Space Administration, 07 Apr 2002. <http://spaceflight.nasa.gov/shuttle/reference/shutref/verboseindex.html>
24. "SIGI - Space Integrated GPS/INS." *Honeywell*. Honeywell International, Inc.: 2006.
25. "CT-602 Star Tracker." *Ball Aerospace*. Ball Aerospace & Technologies Corp. http://www.ballaerospace.com/file/media/D0540_CT-602.pdf
26. Christian, John A., Heather Hinkel, Christopher N. D'Souza, Sean Maguire, and Mogi Patangan. "The Sensor Test for Orion RelNav Risk Mitigation (STORRM) Development Test Objective." *American Institute of Aeronautics and Astronautics*: 2011.
27. "ACE Remote Interface Unit (ACE-RIU)." *ASTi Support*. Advanced Simulation Technology, Inc.: 2013. http://support.asti-usa.com/hardware/ace_riu.html
28. "Advanced, Light-weight, Low-cost Head-up Display System." SAAB Group. SAAB AB: 2014. <http://www.saabgroup.com/Global/Documents%20and%20Images/Air/Avionics%20Systems/RIGS/RIGS%20product%20sheet.pdf>
29. "Integrated S-Band Transponder (ISBT)." Thales Group. Thales Alenia Space. <https://www.thalesgroup.com/sites/default/files/asset/document/ISBT.pdf>
30. Chambers, Andrew, and Dan Rasky. "NASA + SpaceX Work Together." *ASK Magazine*. 17 Oct 2010. http://appel.nasa.gov/2010/10/17/40s_space-x.html/
31. Fragola, Joseph R. *Aerospace Failure Data Handbook*. Valador, Inc., 2010.
32. "Flash Mass Memory Unit." SSTL. Surrey Satellite Technology Ltd., n.d. Web. <http://www.sstl.co.uk/getattachment/115a57bc-8b47-4977-9a8f-1b543d02e6ab/Flash-Mass-Memory-unit--FMMU->
33. Wieland, P., C. Hutchens, D. Long, and B. Salyer. United States. National Aeronautics and Space Administration. Final Report on Life Testing of the Vapor Compression Distillation/Urine Processing Assembly (VCD/UPE) at the Marshall Space Flight Center (1993 to 1997). Huntsville, AL: Marshall Space Flight Center, 1998.
34. "Understanding Your Product Through Reliability Modeling." *Reliability Ques*. Vol. 3.2 Quanterion Solutions Incorporated: 2004.
35. Seedhouse, Erik. *SpaceX: Making Commercial Spaceflight a Reality*. New York, NY: Springer, 2013.
36. National Aeronautics and Space Administration. *NASA's Exploration Systems Architecture Study: Final Report*. NASA-TM-2005-214062. November 2005.